Theor Chim Acta (1992) 83: 331–338

Theoretica Chimica Acta

Study on the dynamic resonance of the L-H-L system: H + ClH

Ju Guan-Zhi[1], Bian Wen-Sheng[1], and Ernest R. Davidson[2]

[1] Institute for Theoretical Chemistry, Shandong University, Jinan, People's Republic of China

[2] Department of Chemistry, Indiana University, Bloomington, IN 47405, USA

Received July 21, 1991/Accepted October 31, 1991

Summary. 1-D quantum calculations of reaction probabilities have been carried out for the collinear reaction $H + ClH(v \leqslant 3) \rightarrow HCl(v' \leqslant 3) + H$ using hyperspherical coordinates. A newly fitted potential energy surface based on *ab initio* multireference Cl calculations, which was regarded as the best available PES for the exchange reaction channel of H + HCl, has been used. According to our calculational results, we find that the diagonal reaction probabilities are far larger than the off-diagonal ones except for P_{01}^R and the vibrational adiabatic principle is not well followed for this reaction. The oscillations of the probability curves are also noticed and the weaker dynamic resonances are identified.

Key words: Dynamic resonance – H + HCl

1. Introduction

Studies on the elementary gas-phase kinetics of the H + HCl system have long been the subjects of reports [1, 2], but there are still some problems left unresolved for the H(D) + ClH reaction [1, 3–5]. Recently, a new potential energy surface for H_2Cl system which was suitable for both exchange and abstraction channels and regarded as the best available global surface has been published [5] and this made it possible for reliable dynamic theoretical research.

As far as the exact quantum scattering calculations, most of the effort has been directed towards the 3-D systems during the past decade [6–14], but systems which have been fully studied by the 3-D exact quantum calculations are still rather few. Therefore, the collinear approximation can still be used to provide valuable information as a complementary method, depending both on its simplicity and its applicability for the reactions which favor a collinear configuration for the transition state [6]. In this work, we performed 1-D exact quantum calculations on the newly fitted potential energy surface [5] for the collinear reaction:

$$H + ClH(v \leqslant 3) \rightarrow HCl(v' \leqslant 3) + H \tag{1}$$

Although this system has been considered, no dynamic resonance discussion was included [15]. Furthermore, compared with the heavy-light-heavy systems, the

characteristics of the quantum mechanical structure of the reaction probability are not well identified for the light-heavy-light systems [16–19]. So we hope that our calculational results can help to understand the dynamic nature of the L-H-L systems.

2. Computational methods

According to the Born–Oppenheimer approximation, the nuclear motion Schrödinger equation, after the removal of the mass center of the system, can be written as Eq. (2) in Delves [20] scaled coordinates:

$$\left[-\frac{1}{2\mu}\left(\frac{\partial^2}{\partial R_i^2}+\frac{\partial^2}{\partial r_i^2}\right)+V(R_i, r_i)-E\right]\Psi(R_i, r_i)=0 \tag{2}$$

where

$$\mu=(m_A m_B m_C/M)^{1/2}$$

$$M=M_A+M_B+M_C$$

Let us introduce the hyperspherical coordinates [14]:

$$\varrho=(R_i^2+r_i^2)^{1/2}$$

$$\alpha=\tan^{-1}(r_i/R_i)$$

where ϱ represents the hyperspherical radius, and α is the hyperspherical angle. They are defined in the intervals:

$$0\leqslant\varrho\leqslant\infty$$

$$0\leqslant\alpha\leqslant\alpha_{\max}\equiv\tan^{-1}[M_B M/M_A M_C]$$

Then, in the new coordinates, the nuclear motion Schrödinger equation (2) becomes:

$$\left[-\frac{1}{2\mu}\left(\frac{\partial^2}{\partial\varrho^2}+\frac{1}{\varrho}\frac{\partial}{\partial\varrho}+\frac{1}{\varrho^2}\frac{\partial^2}{\partial\alpha^2}\right)+V(\alpha, \varrho)-E\right]\Psi(\alpha, \varrho)=0 \tag{3}$$

To solve Eq. (3), the potential is divided into many small sectors by means of the points $\varrho_0, \varrho_1, \ldots, \varrho_{i-1}, \varrho_i, \ldots, \varrho_n$. In the range of ϱ_{i-1} to ϱ_i, $\bar{\varrho}_i$ is chosen as the mean value of them. Then Eq. (3) becomes:

$$\left[-\frac{1}{2\mu\bar{\varrho}_i^2}\frac{\partial^2}{\partial\alpha^2}+V(\alpha, \bar{\varrho}_i)-\epsilon\right]\phi(\alpha, \bar{\varrho}_i)=0 \tag{4}$$

At $\alpha=0$ and $\alpha=\alpha_{\max}$, the eigenfunctions of Eq. (4) satisfy:

$$\phi(0, \bar{\varrho}_i)=\phi(\alpha_{\max}, \bar{\varrho}_i)=0 \tag{5}$$

and form an orthonormal and complete set $\{\phi(\alpha, \bar{\varrho}_i)\}$. In terms of $\phi(\alpha, \bar{\varrho}_i)$, $\Psi^n(\alpha, \varrho)$ can be expanded as:

$$\Psi^n(\alpha, \varrho)=\varrho^{-1/2}\sum_{n'=0}^{N} G_{n'}^n(\varrho, \bar{\varrho}_i)\phi_{n'}(\alpha, \bar{\varrho}_i) \tag{6}$$

By substituting Eq. (6) into Eq. (3), multiplying by $\phi_n^*(\alpha, \bar{\varrho}_i)$ and integrating over the angle α in both sides, the following coupled differential equations can be

obtained:

$$\left[-\frac{1}{2\mu}\frac{d^2}{d\varrho^2}+U(\varrho,\bar{\varrho}_i)-E\right]G(\varrho,\bar{\varrho}_i)=0 \tag{7}$$

U and E are the interaction potential and energy matrices, respectively, given by:

$$U^n_{n'}(\varrho,\bar{\varrho}_i)=\langle n|V(\alpha,\varrho)-(\bar{\varrho}_i^2/\varrho^2)V(\alpha,\bar{\varrho}_i)|n'\rangle$$

$$E^n_{n'}(\varrho,\bar{\varrho}_i)=\left[E+\frac{1}{8\mu\varrho^2}-(\bar{\varrho}_i^2/\varrho^2)\epsilon_n(\bar{\varrho}_i)\right]\delta_{n'n}$$

The coupled differential Eq. (7) is solved by the R matrix propagation method [23, 24]. The ϱ_n and N are determined according to whether the transition probabilities are convergent or not. At the end of the propagation, these $\{\Psi^n\}$ are numerically projected onto the eigenfunctions of AB and BC; thus, the inelastic and reactive transition probabilities are obtained.

Using the method described above [25], we have written a program and done the calculations for H + HH and Cl + HCl. In our present calculations for H + ClH, six even and six odd basis functions have been used, and two closed channels have been employed to guarantee the convergence of the transition probabilities within 0.01. The transition probabilities have been calculated at nearly 200 energy points. All the calculations are performed on the FACOM-M340S machine of Shandong University.

3. Potential energy surface

Many kinds of PES for the H_2Cl system [26–31] have been constructed since the 1930's, when the oldest analytical PES was proposed and soon extended to the H_2Cl system [26]. However, all of these PESs are semi-classical and not satisfactory when both reaction channels are concerned, before the *ab initio* PES [5] applied in this paper was published. The PES used can be expressed as:

$$V = Vspk + V_b$$

Vspk is referred to an extended-LEPS surface which was obtained by Stern, Persky, and Klein in 1973 [29] and was termed as the GSW surface by them. In 1985, this PES was found to be the most accurate one among 11 semi-classical PES for the abstraction channel [31].

V_b is the barrier term fitted into *ab initio* extended-basis-set multireference configuration interaction calculations with scaled external correlation. The formula and corresponding parameters can be found in the literature [5], in which two kinds of PES are presented, but they are equivalent for the collinear configuration.

Because V reduces very closely to *Vspk* for the abstraction channel, it does not provide new information concerning the abstraction reaction. However, it is the best available PES for the exchange reaction and our calculations are based on it.

4. Results and discussion

The reaction probabilities $P^R_{vv'}$, varying with the total energy E (measured from the bottom of the HCl well) are shown in Fig. 1 for the diagonal transitions

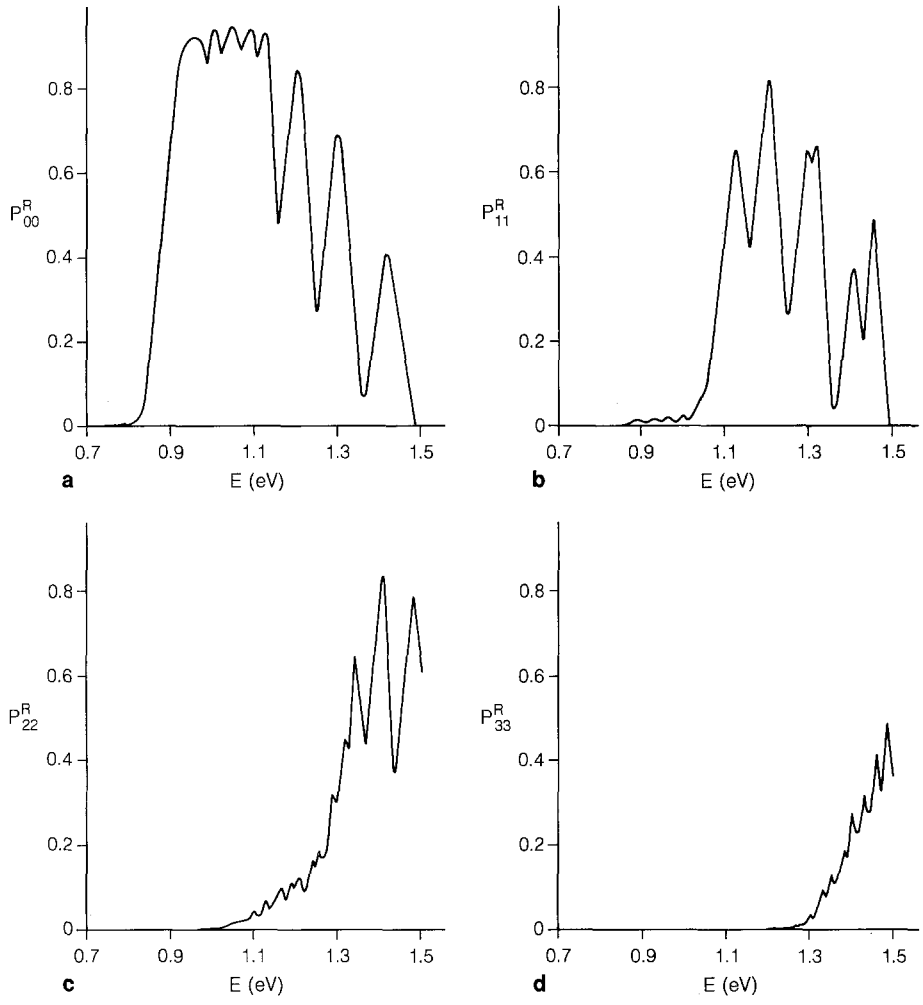

Fig. 1. Reaction probabilities $P^R_{vv'}$ $(v = v')$ as a function of total energy E (measured from the bottom of the HCl well)

$(v = v')$ and in Fig. 2 for off-diagonal ones. The reaction probabilities for $v \neq v' = 3$ are not presented, for P^R_{03} and P^R_{13} are all less than 0.01 and the maximum of P^R_{23} is merely 0.05. We can summarize some features of the reaction probabilities as follows:

1. (a) At $E = 0.19$ eV, only the channel $v = 0$ is energetically open, with a negligible transition probability. The probabilities remain very small until $E = 0.80$ eV and considering the accuracy of our calculations and the literature [32], we assume 0.01 (for the probability) as the indication that a reaction happens. Then we know that the threshold of H + ClH reaction is near 0.82 eV, which is higher [25, 33] than that (0.66 eV) of Cl + HCl.

(b) The energy at which the channel $v = 1$ is also open is found to be 0.54 eV, and 0.88, 1.21 eV are the energies, respectively, at which $v = 2, 3$ are

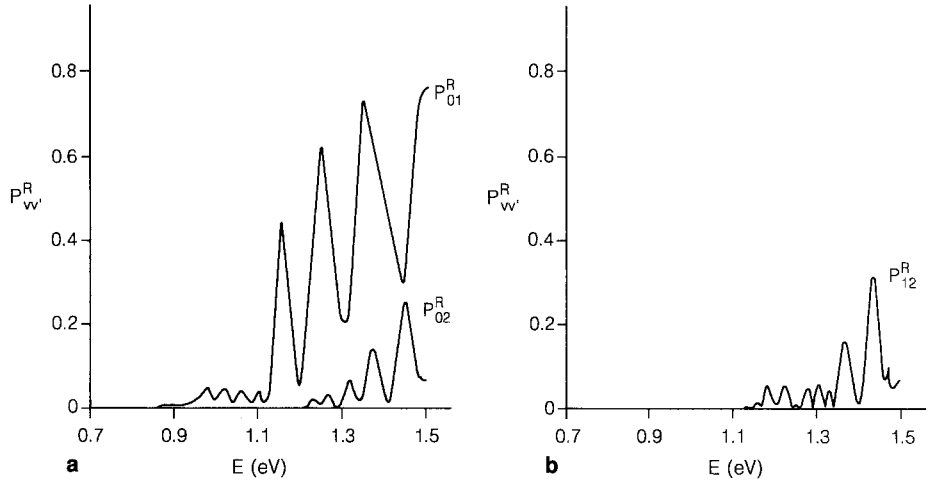

Fig. 2. Reaction probabilities $P^R_{vv'}$ $(v \neq v')$ as a function of total energy E (measured from the bottom of the HCl well)

open. We note that these open energies for H + ClH are identical to those [25] for Cl + HCl and they are very near to the vibrational energy levels of HCl which are 0.1855, 0.5565, 0.9275, and 1.2296 eV subsequently. So it can be concluded that the open energy for the v channel is mainly controlled by the vth vibrational energy level of the reaction species (BC).

(c) When E comes to 1.50 eV, the channel $v = 4$ begins to be opened, and in order to keep two closed channels, we have to restrain the range of the total energy to be less than 1.50 eV.

2. From Fig. 2, we can see that the vibrationally adiabatic principle of the reaction probability is not well followed and the off-diagonal transition P^R_{01} is large. For the H-L-H systems [33–35], the vibrationally adiabatic nature of the reactions results from the conservation of the kinetic energy and this is not the case for the L-H-L systems. In this respect, our conclusion is in agreement with that [16] for H + FH and is reasonable. But the various transitions still exhibit a large vibrationally adiabatic property. Figures 1 and 2 show us that the off-diagonal transitions P^R_{02} and P^R_{12} are far less than the diagonal transitions, let alone P^R_{03}, P^R_{13}, and P^R_{23}. Even P^R_{01} is not as large as P^R_{00}, P^R_{11}, and P^R_{22}. Besides these, the off-diagonal transitions $(v \to v' = v - 1)$ are much preferred to other off-diagonal transitions, i.e., $P^R_{01} \gg P^R_{02}$, $P^R_{23} \gg P^R_{03}$ and P^R_{13}, which also shows some adiabatic character.

3. Whether diagonal or off-diagonal transitions are concerned, the reaction probabilities exhibit many oscillations. Almost all the oscillations occur near the energies, 1.15, 1.25, 1.35, and 1.45 eV. For instance, the P^R_{00} plot has three oscillations at 1.15, 1.25, and 1.35 eV, respectively, and the widths are in the order, 0.04, 0.05, and 0.06 eV. From Figs. 1 and 2, we can also see that the oscillations slightly strengthen as v increases. We tend to attribute these oscillations to the dynamic (Feschbach) resonances and in the next part, we will discuss this in detail.

5. Analysis of the dynamic resonance

5.1. Vibrational non-adiabaticity

Some explanations for the dynamic resonance were made by Levine [36], Kuppermann [21], and Truhlar [18]. It was suggested that the resonances are due to strong coupling terms, corresponding to vibrational non-adiabaticity.

The eigenvalues $\epsilon_{vg}(\varrho)$ and $\epsilon_{vu}(\varrho)$ have been obtained numerically by solving Eq. (4) and their changes with ϱ are shown in Fig. 3. It can be seen that $\epsilon_{vg}(\varrho)$ and $\epsilon_{vu}(\varrho)$ are degenerate and correspond to the vibrational state of HCl at large values of ϱ. As there is only a platform in the interaction region along the curve of $\epsilon_{2g}(\varrho)$, the curves for $v = 0, 1, 2$ can all be regarded as repulsive. But as v increases, three wells appear which belong to ϵ_{3g}, ϵ_{4g}, and ϵ_{5g}, respectively. These wells support this idea that vibrational non-adiabatic couplings lead to the internal excitation resonances. From Fig. 1, we can see that the first resonance is at about 1.15 eV. This energy is near the threshold (about 1.13 eV) of the vibration which is trapped in the shallow well of the ϵ_{3g} curve. Considering non-adiabaticity, the energy can flow into the internal vibrational degrees from the degree of the reaction coordinate in the saddle point region, so at about 1.15 eV, energy can be trapped in or released from the bound states which are supported by the well of ϵ_{3g} curve and this process leads to the first resonance of P_{00}^{R} in Fig. 1a. Furthermore, we are inclined to attribute the other two resonances found at about 1.25 eV and 1.35 eV in Fig. 1a to the other two wells of Fig. 3. This viewpoint has some trouble in explaining why the differences of resonance energies are not as large as the energy intervals between different wells. We suppose that this kind of phenomenon arises from the interference of

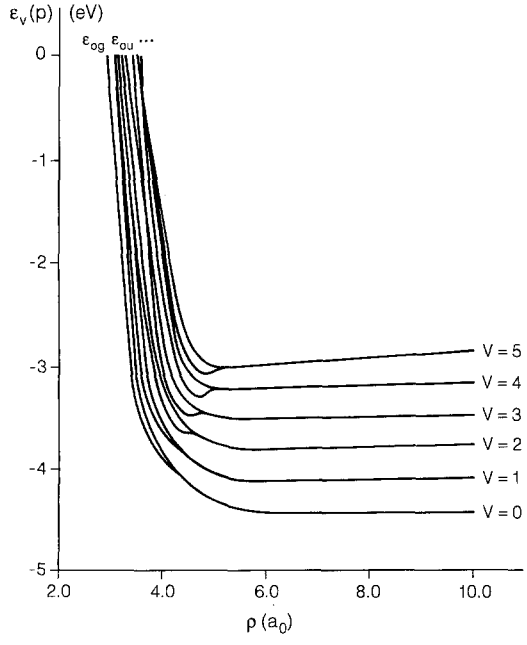

Fig. 3. Eigenvalue ϵ_v as a function of ϱ. Where ϵ_{vg} and ϵ_{vu} are symmetric and asymmetric states

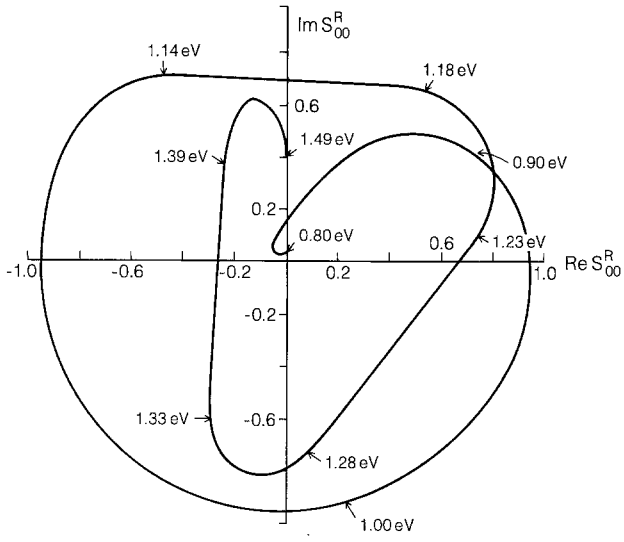

Fig. 4. Argand diagram of Im S_{00}^R versus Re S_{00}^R with the energy E as a parameter

different eigenstates. Resonances in Figs. 1b, 1c, 1d, and Fig. 2 appear also in the vicinity of 1.15, 1.25, 1.35 eV and other higher energies, thus they can be explained similarly.

5.2. Argand diagram

As an example, we draw the Argand diagram for the case: $v = v' = 0$ in Fig. 4. This sort of diagram was shown to be useful in distinguishing a dynamic resonance [17, 18, 37].

The plot in Fig. 4 is traversed in a clockwise direction as ϵ increases, but in the total energy intervals from 1.14 to 1.18 eV, 1.23 to 1.28 eV, and 1.33 to 1.39 eV, it loses most of its curvature, becoming very straight. The three straight lines are due to the effects of three resonances which are not strong enough to change the sign of the curvature leading to a resonance circle and are corresponding to the three minima in Fig. 1a and three wells in Fig. 3. This line of thinking is confirmed by the agreement of energies, at which resonances in Fig. 1a, wells in Fig. 3 and straight lines in Fig. 4 appear.

6. Conclusions

The quantum mechanical structures of the reaction probabilities for transitions, $v(\leqslant 3) \rightarrow v'(\leqslant 3)$, are presented and many weaker dynamic resonances are found for H + ClH systems.

According to the calculational results of present work and those of HFH and HDH [11, 12], we know that the phenomenon of dynamic resonance is common for the L-H-L systems. But these resonances are weaker and often have different structures compared with those of the H-L-H systems [25–27]. Take P_{00}^R as an example. Resonances usually appear at the hind part of the probability curve

and in the shape of valleys for the L-H-L systems, but they are at the front part of the curve which are not far away from the reaction threshold and in the shape of peaks for the H-L-H systems. It is likely that the above situation should result from the fact that in the interaction region, the configuration of H-L-H is more stable than that of L-H-L. Furthermore, in contrast to the case for the H-L-H systems, the vibrationally adiabatic principle of the reaction probability is not well established for the L-H-L systems.

References

1. Thompson DL, Suzukava, Jr. HH, Raff LM (1975) J Chem Phys 62:4727
2. Laidler KJ (1987) Chemical kinetics. 3rd ed. Harper and Row, NY, p 288
3. Weston Jr. RE (1979) J Phys Chem 83:61
4. Miller JC, Gordon RJ (1983) J Chem Phys 78:3713
5. Schwenke DW, Tucker SC, Sleckler R, Brow FB, Lynch GC, Truhlar DG, Garrett BC (1989) J Chem Phys 90:3110
6. Baer M (1985) Theory of chemical reaction dynamics. Vol. 1. CRC Press, Inc, Boca Raton, Florida
7. Kress JD, Pack RT, Parker GA (1990) Chem Phys Lett 170:306
8. Launay JM, Lepetit B (1988) Chem Phys Lett 144:346
9. Cuccaro SA, Hipes PG, Kuppermann A (1989) Chem Phys Lett 154:155
10. Schatz GC (1988) Chem Phys Lett 150:92
11. Truhlar DG, Schwenke DW, Kouri DJ (1990) J Chem Phys 94:7346
12. Webster F, Light JC (1989) J Chem Phys 90:300
13. Zhang JZH, Yeager DL, Miller WH (1990) Chem Phys Lett 173:489
14. Manopoulos DE, Clary DC (1989) Annu Reports C86:95
15. Clary DC (1982) Chem Phys 71:117
16. Schatz GC, Kuppermann A (1980) J Chem Phys 72:2737
17. Kuppermann A (1981) in: Truhlar DG (ed) Potential energy surfaces and dynamics calculations. Plenum, NY, p 375
18. Garrett BC, Truhlar DG, Schatze GC, Walker RB (1981) J Chem Phys 85:3806
19. Clary DC (1983) J Chem Phys 78:777
20. Delves LM (1959) Nucl Phys 9:391; ibid, (1960) 20:275
21. Kuppermann A, Kaye JA, Dwyer JP (1980) Chem Phys Lett 74:257
22. Hauke J, Manz J, Römelt J (1980) J Chem Phys 73:5040
23. Light JC, Walker RB (1976) J Chem Phys 65:4272
24. Stechel EB, Schatz JG, Light JC (1979) J Chem Phys 70:5640
25. Ju GJ, Chen DZ (1989) Acta Chim Sinica, English Edition 6:496
26. Wheeler A, Topley B, Eyring H (1936) J Chem Phys 4:178
27. Bigeleisen J, Klein FS (1959) J Chem Phys 30:1340
28. Parr CA, Truhlar DG (1971) J Chem Phys 75:1844
29. Stern MJ, Persky A, Klein FS (1973) J Chem Phys 58:5697
30. Garrett BC, Truhlar DG, Magnuson AW (1981) J Chem Phys 74:1029
31. Tucker SC, Truhlar DG, Garrett BC, Isaacson AD (1985) J Chem Phys 82:4102
32. Manz J, Schor HHR (1984) Chem Phys Lett 107:549
33. Bondi DK, Connor JNL, Manz J, Römelt J (1983) Mol Phys 50:467
34. Baer M (1975) J Chem Phys 62:305
35. Hiller C, Manz J, Miller WH, Römelt J (1983) J Chem Phys 78:3850
36. Levine RD, Wu S (1971) Chem Phys Lett 11:557
37. Schatz GC, Kuppermann A (1973) J Chem Phys 59:964